Environmental Earth Sciences (2018) 77:211
https://doi.org/10.1007/s12665-018-7384-8

THEMATIC ISSUE

Geochemical and mineralogical composition of black weathering crusts on limestones from seven different European countries

Orsolya Farkas[1] · Siegfried Siegesmund[2] · Tobias Licha[3] · Ákos Török[1]

Received: 3 November 2017 / Accepted: 24 February 2018 / Published online: 6 March 2018

Abstract

Twenty-seven samples of black weathering crust and host carbonates were studied from seven European countries (Germany, Hungary, Belgium, Czech Republic, France, Italy and Poland) representing 11 different sites. The samples were collected for sites for which long-term air pollution records are available. The mineralogical analyses (XRD, polarizing microscopy, SEM) have shown that despite decreasing SO_2 emissions crust samples are still very rich in gypsum. Further, in all host rock samples gypsum was also detected. Good correlations ($R^2 > 0.9$) were also found between water-soluble calcium and gypsum content and between sulphate and gypsum content both for black crusts and host rocks. The black gypsum crusts are four or five times richer in sulphate than the host rock. The conductivity of dissolved crust and host rock samples also shows a positive correlation with gypsum content of the samples. LA-ICP-MS analyses allowed the detection of high Pb-levels in black crusts and a negative shift in lead concentration at the crust/host rock transition. The lead content of the host rock is 2–5 mg/kg, while that of the crust is 3–25 mg/kg in the sample collected from Germany, while in the Belgian sample these values are 2–14 mg/kg and 80–870 mg/kg for the host rock and crust, respectively. The GC–MS technique allowed to detect the PAH content of black crusts and host rocks. The former one contains 0.6–15.6 (102.5) mg/kg, while in the host rock values between 0.2 and 2.4 mg/kg were found. The present study suggests that still large amounts of air pollution-related minerals and organic pollutants are found in the black weathering crusts of European carbonate buildings despite decreasing trends in air pollution.

Keywords Stone decay · Black weathering crust · Sulphate · Gypsum · Air pollution · Air quality · SO_2 concentration · Airborne organic pollutants

Introduction

Air pollution-related stone deterioration has been investigated from the beginning of the twentieth century (Kaiser 1910; Grün 1931, Kieslinger 1932, Schaffer 1932). Fitzner et al. 1996 classified the weathering forms and defined damage categories. The most frequently observed type of surface deterioration is crust. These crusts form in rain-exposed as well as in rain-protected areas. The former contains a high proportion of biological matter (Snethlage 2008), and the latter consists mainly of gypsum (Del Monte et al. 1981). The crust formation is also considered an accumulation of materials on the stone surface. In this approach, crusts are also divided to black crust and salt crust according to ICOMOS (2008). The interaction of acid rain and stone substrate also leads to crust formation. Thus, crusts can be formed by exogenic deposits in combination with materials derived from the stone. The process of crust formation

This article is part of a Topical Collection in Environmental Earth Sciences on "Stone in the Architectural Heritage: from quarry to monuments—environment, exploitation, properties and durability", guest edited by Siegfried Siegesmund, Luís Sousa and Rubén Alfonso López-Doncel.

✉ Orsolya Farkas
farkas.orsolya@epito.bme.hu

[1] Department of Engineering Geology and Geotechnics, Budapest University of Technology and Economics, Műegyetem avenue 3-5, Budapest 1111, Hungary

[2] Department of Structural Geology and Geodynamics, Geoscience Center of the University Göttingen, Goldschmidtstraße 3, 37077 Göttingen, Germany

[3] Department of Applied Geology, Geoscience Center of the University Göttingen, Goldschmidtstraße 3, 37077 Göttingen, Germany

and the damage on carbonate rock materials are described in detail in the past (Amoroso and Fassina 1983; Baboian 1986; Brimblecombe 1987, 1996, 2003; Rosvall and Aleby 1988, Winkler 1994; Price 1996; Camuffo 1998; Charola 2001; Charola and Ware 2002; Sabbioni 1995). It is clear from these papers that acid rain dissolves carbonate substrate which invokes the formation of free calcium ions that react with sulphur of the wet deposits, and thus lead to gypsum formation.

In the case of limestone, it is also recognized that the main stone deterioration processes are gypsum formation and carbonate dissolution (Sabbioni 2003). Gypsum (calcium sulphate, $CaSO_4*2H_2O$) is formed from the reaction/interaction of calcium carbonate (the main rock-forming mineral of limestone: calcite, $CaCO_3$) with atmosphere-derived sulphur oxides (SO_x). During dissolution and re-precipitation of carbonate, other compounds are trapped, especially settled dust, and thus catalyzing gypsum crust formation and causing discoloration from grey to black (Rodriguez-Navarro and Sebastian 1996; Ausset et al. 1999). The gypsum is formed on the stone surface and below, within the pores of the rock (Del Monte et al. 1981; Amoroso and Fassina 1983). The morphology of black crusts shows some varieties from thin laminar crusts or black crusts tracing the surface (Moropoulou et al. 1998; Török 2003; De Kock et al. 2017) to globular or framboidal crusts (Del Monte et al. 1981; Török 2002). The microstructural characterization of the black crusts developed significantly from optical microscopy (Moropoulou et al. 1998; Török 2003, Pozo-Antonio et al. 2017) to scanning electron microscopy (Ausset et al. 1999; Smith et al. 2003) and finally to computer tomography (De Kock et al. 2017) supporting the theory that organic particles have a significant role in black crust formation.

Deterioration of architectural heritage is caused by chemical, physical and biological processes and very often related to air pollution. It is generally accepted that there is a correlation between chemical composition of crust and air pollution (Ausset et al. 1999; Maravelaki-Kalaitzaki and Biscontin 1999; Bonazza et al. 2004; Török 2008; Urosevic et al. 2012; De Kock et al. 2017). Based on microscopic and elemental analysis, gypsum crusts contain, in addition to the aforementioned dust wind, drifted mineral particles (Smith et al. 2003) and various types of organic matter (Fobe et al. 1995; Török and Rozgonyi, 2004; Bonazza et al. 2005; Sánchez et al. 2011; Pozo-Antonio et al. 2017). Major and trace elements (Gavino et al. 2004) and also isotopic compositions of damaged and discoloured layers were reported (Torfs and Van Grieken 1997; Klemm and Siedel 2002; Siegesmund et al. 2007).

The weathering crusts consist of newly formed minerals, porous carbonaceous particles (soot), smooth aluminosilicate particles and metal particles mainly composed of iron (Del Monte et al. 1981; Esbert et al. 1996; Derbez and Lefèvre 1996). These atmospheric particles are derived from different sources: fuel oil combustion of domestic heating and power plants, coal combustion, gas oil emission (Sabbioni 1995), biomass combustion (Ausset et al. 1992), as well as vehicle exhaust gases (Hildemann et al. 1994; Rodriguez-Navarro and Sebastian 1996; Slezakova and Castro 2011).

Several papers have dealt with marble (Moropoulou et al. 1998; Maravelaki-Kalaitzaki and Biscontin 1999), and various types of limestone monuments (Amoroso and Fassina 1983; Viles 1993; Fobe et al. 1995; Török 2002; Gavino et al. 2004; Smith and Viles 2006; McAlister et al. 2006; Siegesmund et al. 2007; Török et al. 2007) are found in urban areas; however, only few researches have compared the black crust formation of stone buildings from rural and urban areas (Török et al. 2011; Graue et al. 2013).

The present paper follows this line (papers by Török et al. 2011 and Graue et al. 2013) with a broader sampling campaign covering seven countries in Europe. Buildings that were constructed from carbonates (mostly limestone) were studied. Black weathering crusts were collected from those buildings or stone structures, and their mineralogical–geochemical composition was analysed in order to compare compositional differences with air pollution scenarios. Microscopic analyses (plane-polarized light, cathodoluminescence and scanning electron microscopy (SEM)) were used to characterize textural differences between samples. Special emphasis was placed on the amount of gypsum in weathering crusts and host rocks together with the proportion of sulphate in these samples. Conductivity of samples extracted with deionized water was compared to the gypsum content. Lead content and accumulation of polycyclic aromatic hydrocarbon (PAH) in weathering crusts and host rocks were also analysed allowing to distinguish between crust and rock. The aims of these complex analyses were to have a broad overview of black crust formation on limestone in environments that have different pollution fluxes and to outline the similarities of crust formation on carbonate substrate.

Materials and methods

Samples and environmental conditions

The black weathering crust and host carbonate rock samples were collected from seven European countries: Germany (D), Hungary (H), Belgium (B), Czech Republic (CZ), France (F), Italy (I) and Poland (PL) (Table 1). The study sites are mostly located in continental climate in Western and Central Europe, with minor oceanic influence at sites in Belgium and France. Relatively dry climate with hot summers and cold winters is typical. The mean annual temperature ranges between 8.6 and 10.4 °C for the studied

Table 1 Climate, geography and some data on the population of sites from where the samples were taken (DWD—Deutscher Wetterdienst 2016; Wetterkontor 2016; CHMI 2017; Climate-Data 2017; WMO—UN World Meteorological Organisation 2017)

Description of sampling sites	Halberstadt	Naumburg (Saale)	Braunschweig	Gottingen	Letmathe	Budapest	Liege	Brno	Reims	Bari	Katowice
Country code	D	D	D	D	D	H	B	CZ	F	I	PL
Mean annual temperature [°C]	8.8	8.9	8.8	8.7	8.9	10.4	9.8	9.4	10.2	15.8	8.6
Annual precipitation [mm]	542	523	621	644	973	593	827	505	598	586	686
Warmest month [°C]	Jul	Jul	Jul	Jul	Jul	Jul	Jul	Jul	Jul	Jul	Jul
	22.6	23.1	17.5	17.1	21.6	20.8	22.3	24.5	23.9	28.4	24.5
Coldest month [°C]	Feb	Feb	Jan	Jan	Jan	Jan	Jan	Jan	Jan	Jan	Jan
	− 2.4	− 2.3	− 0.2	0.3	− 0.5	− 1.6	− 0.3	− 5.2	− 0.6	5.0	− 6.6
Metres above sea level [m]	122	130	75	150	247	315	66	237	106	5	266
Total area [km^2]	143.0	129.9	192.2	116.9	35.4	525.1	69.4	230.2	46.9	116.0	164.6
Total population [capita]	43,768	33,012	251,364	118,914	25,524	1,757,618	196,970	377,973	183,042	324,198	298,111
Population density [capita/km^2]	306	254	1308	1017	721	3350	2839	1642	3903	2795	1811

cities (Table 1). One exception is Bari (Italy), which has a Mediterranean climate characterized by warm, dry summers and rainy, mild winters. Annual precipitation is between 500 and 700 mm, except Liege and Letmathe with more than 800 mm.

The samples were mainly collected from urban areas; however, the size of these settlements is very different from small cities with less than 50,000 inhabitants (Letmathe, Naumburg and Halberstadt); medium ones with population of 100,000 and 200,000 (Göttingen, Liege and Reims), 250,000–350,000 (Braunschweig, Brno, Bari and Katowice); or big cities like Budapest with inhabitants of 1.8 million people.

Not only rural (with small cities and cleaner surrounding) and urban regions were selected, but also industrial areas. Some sampling sites are located close to coal power stations (Fig. 1).

The recent and historic air quality in these seven countries is different. Focusing on SO_2 concentrations, a significant decrease from the mid-1990s was observed. However, there are some countries where this trend has now stopped. Germany, Belgium and Hungary are nowadays in much better position than in the 1990s. Although Poland has achieved a significant decrease in the immission of SO_2, it is still higher than that of the other countries (Fig. 2).

The reduction in total SO_2 and PM_{10} emission is clear at national levels (Table 2). Between 1990 and 2000, the SO_2 emissions significantly dropped. The reduction is almost double in terms of SO_2, than of PM_{10} from 2000 to 2015 in Germany, Belgium, France and Poland, and the values are four times lower in Italy. Nearly 40% of the reduction in PM_{10} was measured in the Czech Republic. Unfortunately, in Hungary the situation is completely different, although the greatest reduction in SO_2 (94%) was recorded, but PM_{10} emission slightly increased in the past years.

The above-listed values further depend on the size of the country; therefore, a relative indicator was also calculated. In Poland and in Czech Republic, this value is more than 10 (18.2 and 11.7 kg SO_x emission/capita), despite the medium to small population (Fig. 3). Italy and France are good examples, since the number of inhabitants is high, but the emission levels are acceptable. The indicator has lower values 2.0 and 2.3, respectively. Hungary has a smaller population and lower emissions with an indicator value of 2.4.

In total, 27 samples (13 weathering crusts and 13 host rocks and 1 sample that contained both crust and host rock) were collected mostly from limestone buildings throughout Europe from 11 sites. Two-thirds of the samples were taken from historic buildings (churches, public buildings), while the rest of the samples were picked from stone walls or one from a natural cliff (Table 3). Samples were taken at least 1.5 m above the ground level to avoid the influence of deicing salts and other external factors (e.g. urine) and soil

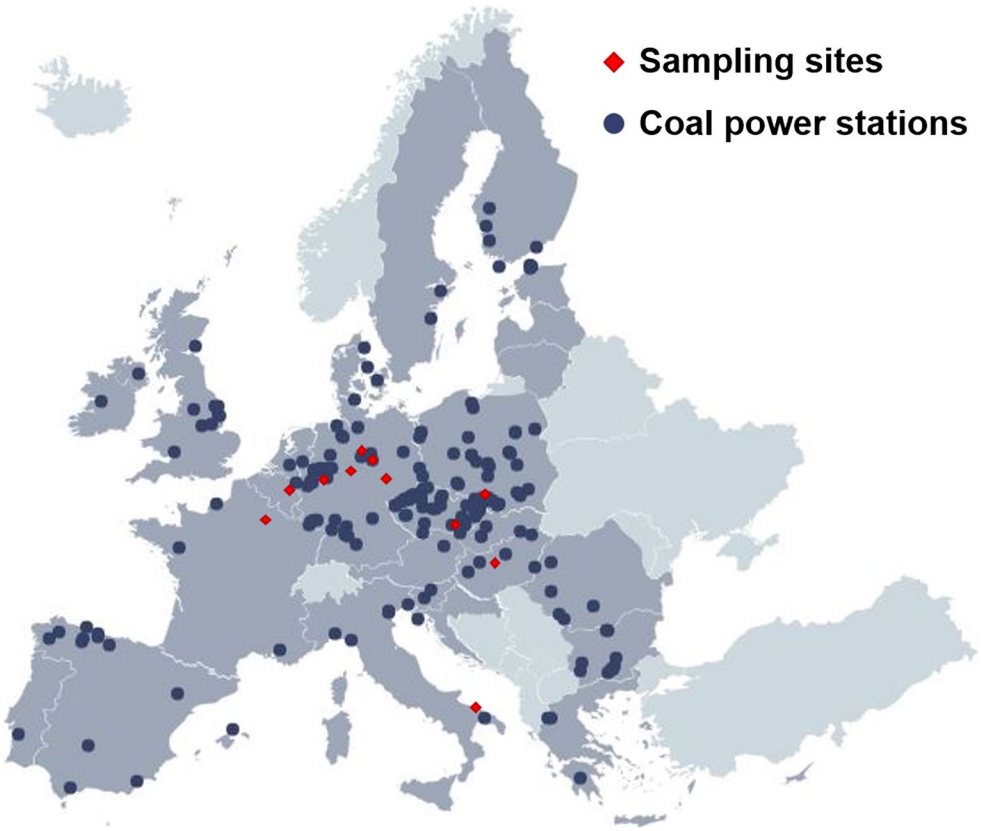

Fig. 1 Location of sampling sites and 30 years and older operational coal power stations in Europe (based on the Coal Map of Europe—CAN 2015) (list of samples is given in Table 3)

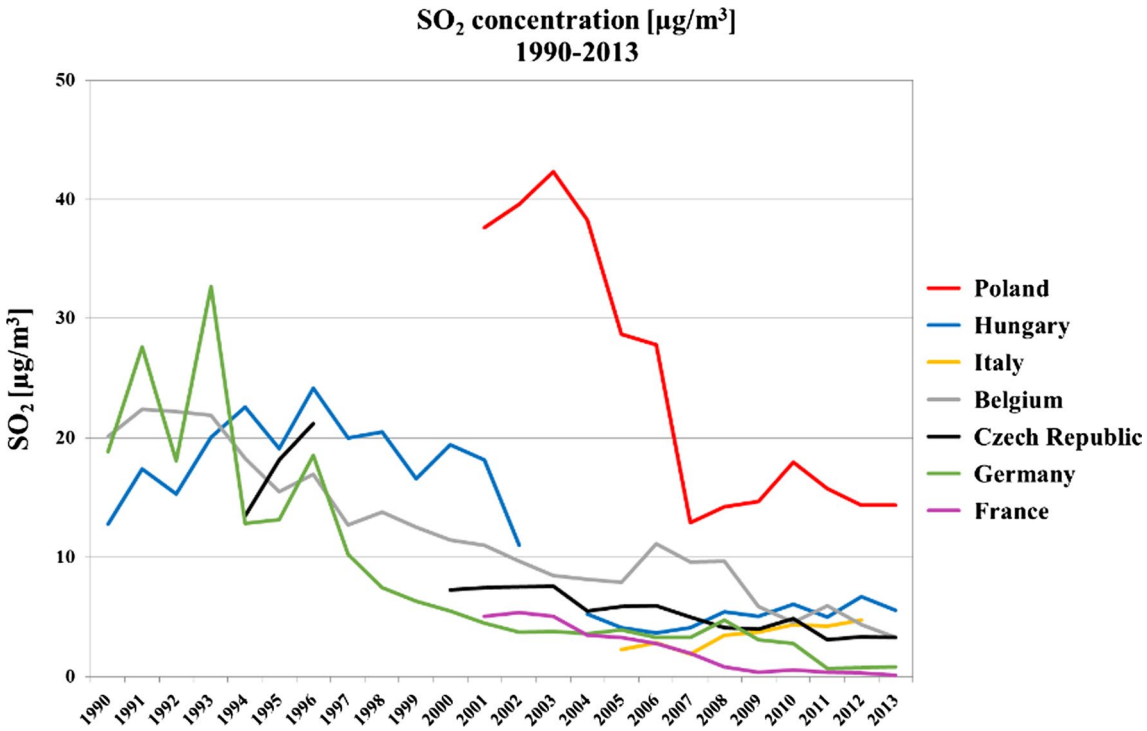

Fig. 2 Annual mean concentrations of sulphur dioxide (SO_2) 1990–2013 in the nearest air quality monitoring stations (based on European Environment Agency (EEA) dataset (EEA—EU European Environment Agency 2016a) and interactive SO_2 maps (EEA—EU European Environment Agency 2016b) on the following stations: Göttingen (DENI042); Naumburg (DEST078); Halberstadt (DEST009-044); Braunschweig (DENI011); Budapest–Baross (HU0005A) & Teleki (HU0045A); Liege (BETH201); Brno-Turany (CZ0BBNY); Reims (FR14004); Bari (IT1606A); Katowice (PL0008A)

Table 2 SO_2 and PM_{10} national total emissions [Gg] in selected countries (D: Germany, H: Hungary, B: Belgium, CZ: Czech Republic, F: France, I: Italy and PL: Poland) in the years 1990, 2000 and 2015 and the rate of emissions in the year 2015 [%] based on 1990 (SO_2) and 2000 (SO_2, PM_{10}) (Data source: EEA)

	D	H	B	CZ	F	I	PL
SO_2 emission [Gg] (1990)	5485	825	365	1871	1314	1783	2648
SO_2 emission [Gg] (2000)	644	428	173	227	631	755	1404
SO_2 emission [Gg] (2015)	352	24	43	123	153	123	690
PM_{10} emission [Gg] (2000)	290	69	57	56	449	225	271
PM_{10} emission [Gg] (2015)	221	70	38	35	266	179	221
SO_2 emission—2015 [%] based on 1990	6%	3%	12%	7%	12%	7%	26%
SO_2 emission—2015 [%] based on 2000	55%	6%	25%	54%	24%	16%	49%
PM_{10} emission—2015 [%] based on 2000	76%	101%	65%	62%	59%	79%	82%

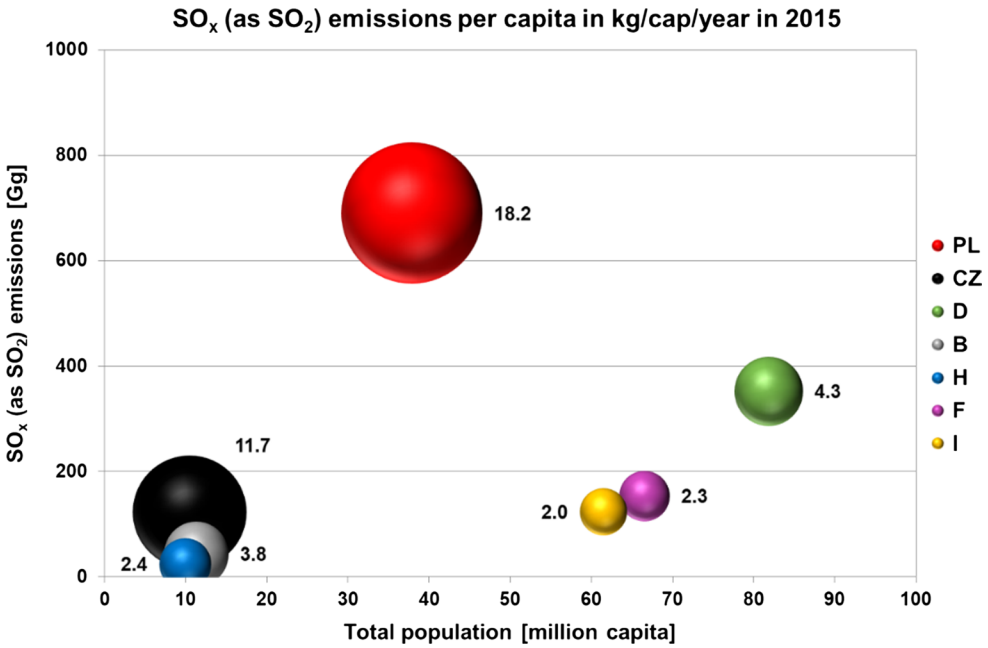

Fig. 3 SO_x (as SO_2) emissions versus population in 2015 in the countries from where samples were collected (PL: Poland, CZ: Czech Republic, D: Germany, B: Belgium, H: Hungary, F: France and I: Italy). The size of the bubbles and numbers next to them shows the relative value [kg/capita]

contamination (Fig. 4). Carbonate rocks were selected as a substrate since limestone and marble have a fairly uniform mineralogy (calcite) that interacts with air pollution, in the form of weathering crust formation. Similarly to previous studies, two major types of black crusts were identified: i) laminar and ii) dendritic or globular black crusts. The former one can cover the entire façade and most commonly develops on vertical areas, which are sheltered from direct rain wash (Fitzner et al. 1996). The second type of black crusts—represented by most of the collected samples—are also called globular (Bonazza et al. 2007), ropey (Antill and Viles 1999) or framboidal (Török 2003, 2008) black crusts. This form usually develops on protected and sheltered parts of the building façade, which are not exposed to direct rain wash.

Analytical techniques

Host rock and weathered black crust samples were analysed with eight different methods including plane-polarized light microscopy, cathodoluminescence and scanning electron microscopy, X-ray diffraction (XRD) and laser ablation inductively coupled plasma mass spectrometry (LA-ICP-MS). Aqueous extracts were analysed for conductivity and with ion chromatography. Solvent extracts were analysed using gas chromatography–mass spectrometry (GC–MS) (Table 3).

Fabric analysis of thin sections was performed by polarizing microscopy (ZEISS Axioplan 2 imaging with a PROGRESS C10 camera, Göttingen, Germany).

Prior to cathodoluminescence imaging, thin sections were coated with carbon. A hot-cathode microscope (HC3-LM, Simon-Neuser, Göttingen, Germany) with a coupled Peltier-cooled Kappa PS 40C-285 (DX) camera system (resolution 1.5 mpx) attached to an Olympus BH-2 microscope was used for visualizing internal structures and zoning in minerals. The electron gun was operated at a voltage of 14 keV under high vacuum (10^{-4} bar) with a filament current of 0.18 mA; the diameter of the electron beam was ca. 4 mm. (Neuser et al. 1995).

Table 3 Samples and their description (in sample code letters mean countries (D: Germany, H: Hungary, B: Belgium, CZ: Czech Republic, F: France, I: Italy and PL: Poland))

Sample code	Locality	Saiup dug she	Description of host rock	Sample description	Analytical methods							
					Plane-polarized light M.	Cathodoluminescence M.	Scanning electron M.	Röntgen diffraction	Conductivity	Ion chromatography	LA-ICP-MS	GC-MS
D1-a	Halberstadt (Germany)	Church	Limestone	Host rock	+	−	−	+	+	+	−	+
D1-b				Blade crust			+	+	+	+		+
D2-a	Naumburg (Germany)	Church	Limestone	Host rock	+	−	−	+	+	+	−	+
D2-b				Black crust			+	+	+	+		+
D3-a	Braunschweig (Germany)	Church	Oolitic limestone	Host rock	+	+	−	+	+	+	−	+
D3-b				Black crust with limestone			+	+	+	+		+
D4-a	Göttingen (Germany)	Stone fence	Limestone	Host rock	+	+	−	+	+	+	+	+
D4-b				Black crust			+	+	+	+		+
D5-a	Göttingen (Germany)	Church	Limestone	Host rock	−	−	−	+	+	+	−	+
D5-b				Black crust			−	+	+	+		+
D6-a	Göttingen (Germany)	Stone wall	Limestone	Host rock	−	−	−	+	−	+	−	+
D6-b				Black crust			−	+	+	+		+
D7-a	Iserlohn (Germany)	Natural cliff	Limestone	Host rock	−	−	−	+	−	+	−	+
D7-b				Black crust			−	+	+	+		+
H1-a	Budapest (Hungary)	Historic building	Bioclastic limestone	Host rock	−	−	−	+	+	+	−	+
H1-b				Black crust with limestone			+	+	+	+		+
H2-a	Budapest (Hungary)	Historic building	Bioclastic limestone	Host rock	+	+	−	+	−	+	−	+
H2-b				Black crust			+	+	+	+		+
B-a	Liège (Belgium)	Church	Limestone	Host rock	+	+	−	+	+	+	+	+
B-b				Black crust			+	+	+	+		+
CZ-a	Brno (Czech Republic)	Stone wall	Limestone	Host rock	−	−	−	+	+	+	−	+
CZ-b				Black crust			−	+	+	+		+
F-a	Reims (France)	Church	Oolitic limestone	Host rock	+	+	−	+	−	+	−	+
F-b				Black crust with limestone			+	+	+	+		+
I	Bari (Italy)	Public building	Marble	Black crust with marble	+	+	+	+	−	+	−	+
PL-a	Katowice (Poland)	Stone wall	Travertin	Host rock	+	+	−	+	−	+	−	+
PL-b				Black crust			+	+	+	+		+

"a" represents host rock, while "b" stands for black weathering crust and applied analytical methods (three different types of microscopy (plane-polarized light (PPL), cathodoluminescence (CL) and scanning electron microscopy (SEM)), X-ray diffraction (XRD), measurement of conductivity, ion chromatography (IC), laser ablation inductively coupled plasma mass spectrometry (LA-ICP-MS) and gas chromatography–mass spectrometry (GC–MS) analyses). Measurements were performed with the plus (+) sign

Fig. 4 Sampling sites and collected samples (samples were collected from the framed area). **a**, **b** D2 sample from Wenzelskirche Naumburg, Germany, **c**, **d** D3 sample from Petrikirche Braunschweig, Germany, **e**, **f** H1 sample from Budapest University of Technology and Economics Budapest, Hungary, **g**, **h** D6 sample from Albaniplatz Göttingen, Germany, **i**, **j** D7 sample from Pater & Nonne, Letmathe-Iserlohn, Germany

To visualize the microfabric of the crust, a scanning electron microscope (SEM, Quanta 650-FEG-MLA by FEI Company, Institute of Mineralogy, TU Bergakademie Freiberg/Saxony, Germany) was applied on small fragment samples. The samples were graphite-coated for SEM imaging (LEICA EM MED020). Electron beam conditions were set at 25 kV acceleration voltage and to a 10 nA beam spot.

The mineralogical composition was determined by X-ray diffraction (XRD) with a Philips diffractometer (PW 1800, Cu-anode, 45 kV, 30 mA, Göttingen, Germany). Powder X-ray patterns were obtained using PANalytical X'Pert HighScore Plus. The diffraction data were recorded from 2° to 70° 2Θ via a continuous scan with a routine scan programme. The RockJock program was used for quantitative analysis. RockJock is a computer program that determines

quantitative mineralogy in powdered samples by comparing the integrated X-ray diffraction (XRD) intensities of individual minerals in complex mixtures to the intensities of an internal standard. (Eberl 2003).

Conductivity of solutions (50 mg of pulverized sample dissolved in 50 ml water) was also measured (Multi 340i, Göttingen, Germany).

Ion chromatography (IC) was used in the determination of the water-extractable mineral fractions. Prior to analysis, samples were extracted in a 1:20 and 1:1000 ratio of powdered sample to water (50 mg pulverized host rock samples in 1 ml water, 50 mg pulverized crusts in 50 ml water) in plastic vials for 48 h on a shaker (GFL 3005 shaker, 250 1/min, orbital motion, Göttingen, Germany) at room temperature. Extracts were centrifuged and filtered through a 0.2-µm membrane filter prior to analysis. Major cations were analysed on a DIONEX 320 (Göttingen, Germany) using electrochemically suppressed conductivity detection with ion separation achieved on a CS16 column using methane sulphonic acid as eluent. Major anions were analysed on a DIONEX 500 (Göttingen, Germany) using electrochemically suppressed conductivity detection with ion separation achieved on an AS11-HC column using potassium hydroxide as eluent. The calibration ranges were: for sulphate, 0.5–50 mg/l; calcium, 0.05–10 mg/l; and high values for calcium, 10–150(500) mg/l.

Laser ablation inductively coupled plasma mass spectrometry (LA-ICP-MS) analyses were performed on thin slices of the samples. The laser used was a Compex 110 Excimer (ArF 193 nm) by Lambda Physik (Göttingen, Germany), a GeoLas optical bench by MicroLas (Göttingen, Germany), an ablation pit with a diameter of 33 µm and 5-Hz repetition rate for the laser pulses with 80 mJ. The mass spectrometer was Thermo Fischer Scientific Element 2. Calibration was done using NBS610 (NIST, USA, 2011), internal standard ^{43}Ca, dwell time 10 ms/isotope and 0.995 s per sweep. This study presents the results of ^{34}S and ^{208}Pb. The measuring line consisted of 40 (sample D4) and 35 (sample B1) measuring points with the same resolution of 60 µm.

For polycyclic aromatic hydrocarbon (PAH) analysis, the pulverized host rock samples (250 mg) and black crusts (125/250 mg) were weighted into Teflon vessels, 3 µl internal standard (15 ng/µl) and 2 ml isohexane were added and subsequently extracted on a MARS XPRESS microwave system at 150 °C for 10-min heating time and 40-min holding time (1600 W, 100%). The extraction was repeated. After cooling, the supernatant was removed and transferred into 1.5-ml glass vials. The extracts were analysed using gas chromatography–mass spectrometry (GC–MS, Agilent 7890A, 5975C, Göttingen, Germany). Separation of PAHs was achieved on a VF-17 ms column (Agilent, 30 m length, 0.25 mm inner diameter and 0.25 µm film thickness). Data were recorded in single-ion monitoring mode. The range of the detected 22 PAH compounds is from acenaphthylene (m/z 52) to dibenzo(a,h)pyrene (m/z 302). Data quality was ensured using six internal standards (acenaphthene-d10, phenanthrene-d10, pyrene-d10, chrysene-d12, perylene-d12, benzo(g,h,i)perylene-d12) over the complete method. The limit of quantitation (LOQ) was mainly 1 µg/kg (14 PAH compounds), 2 µg/kg (7 PAHs) and 5 µg/kg (anthracene).

Results

Crust morphology

Scanning electron microscopic analyses revealed that the collected black crusts contain significant amount of gypsum crystals. There is a morphological difference between gypsum crystals of laminar black crusts and framboidal black crusts. The top of the framboidal black crust is characterized by the presence of rosette-like gypsum crystals (Fig. 5). These idiomorphic gypsum crystals form a network that entraps particulates. According to SEM analyses, various types of particulate matter are also present. Carbonaceous particulate matter, iron-rich and silica-rich spherules and mineral fragments were also observed. Particles are partly incorporated into gypsum crystals or partly visible as globular forms attached to the surface of gypsum crystals (Fig. 5e).

We have used cathodoluminescence microscopy (CL) to study these transitions. The CL imaging technique shows that there is a very sharp boundary between the crust and host rock. The limestone substrate usually shows a bright orange luminescence, while the black crust mainly consists of fine-grained non-luminescent parts with scattered few micron-sized orange luminescence spots (Fig. 6). The black crust also displays few isolated spots of violet-blue luminescence. These violet-blue spots are considered silt-sized wind-blown mineral particles such as quartz.

Mineralogy

The sample preparation—separation of crust and host rock (Table 3)—allowed to detect the mineralogical composition of crust and host rock using XRD technique. The RockJock program determines quantitative mineralogy from the integrated X-ray diffraction (XRD) intensities of individual minerals (e.g. calcite, gypsum and quartz). The analytical results are in good correlation with the previous findings, namely in the calcitic host rock only minor amounts of gypsum are found, while in the black crusts gypsum prevails (Table 4). The crust also contains small amounts of quartz.

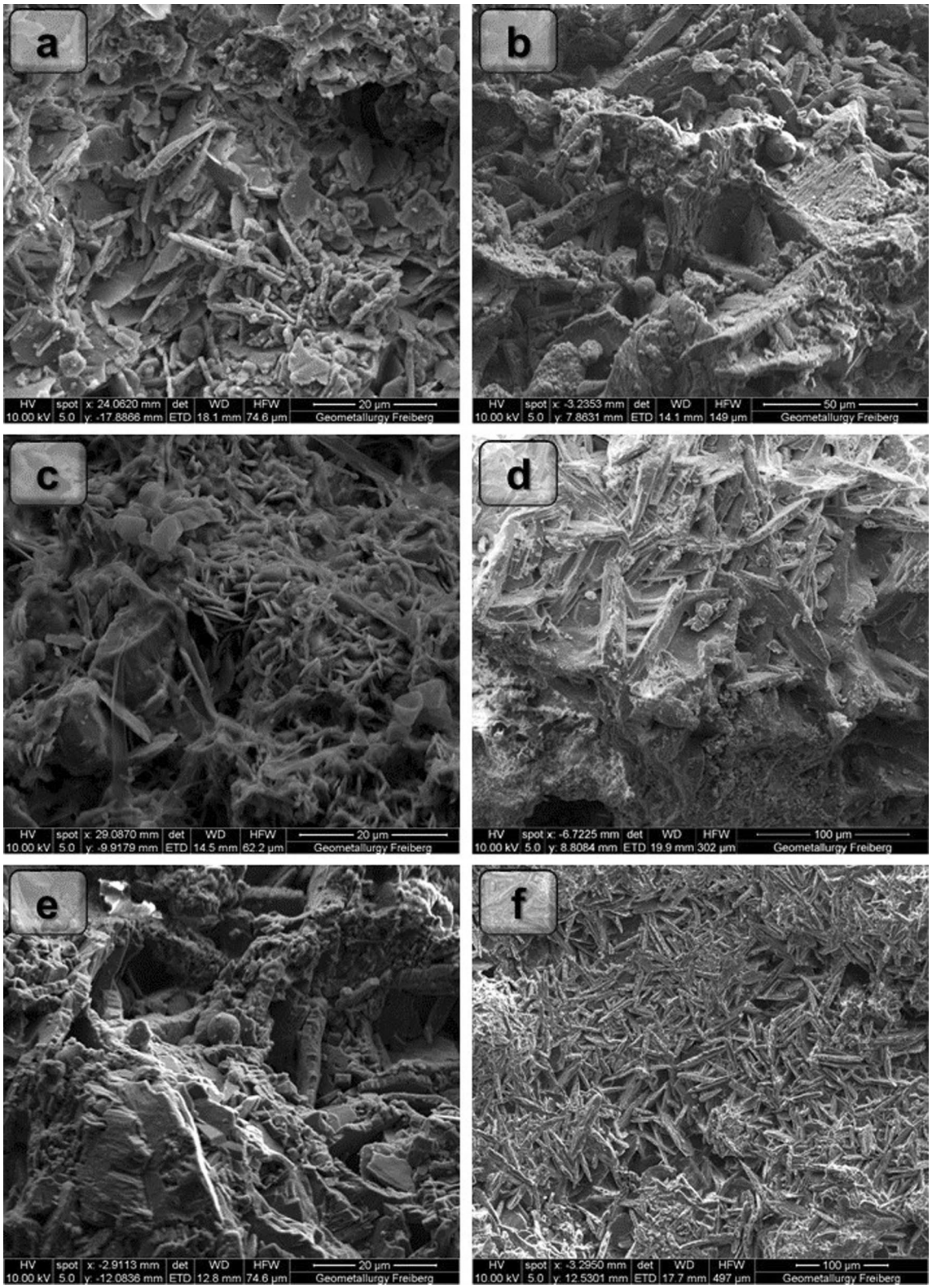

Fig. 5 SEM images of crust samples from Germany **a** rosette-like gypsum crystals on limestone (sample D4, Göttingen Germany); **b** spherical particulate matter entrapped in rosette-like gypsum crystals (sample B, Liege Belgium); **c** various sizes of idiomorphic gypsum rosettes (sample F, Reims France); **d** dense network of tabular gypsum crystals (sample H1, Budapest Hungary); **e** spherical particulate matter (in the centre) entrapped in gypsum crystals (sample PL, Katowice Poland); **f** very dense network of rosette-like gypsum crystals on limestone (sample PL, Katowice Poland)

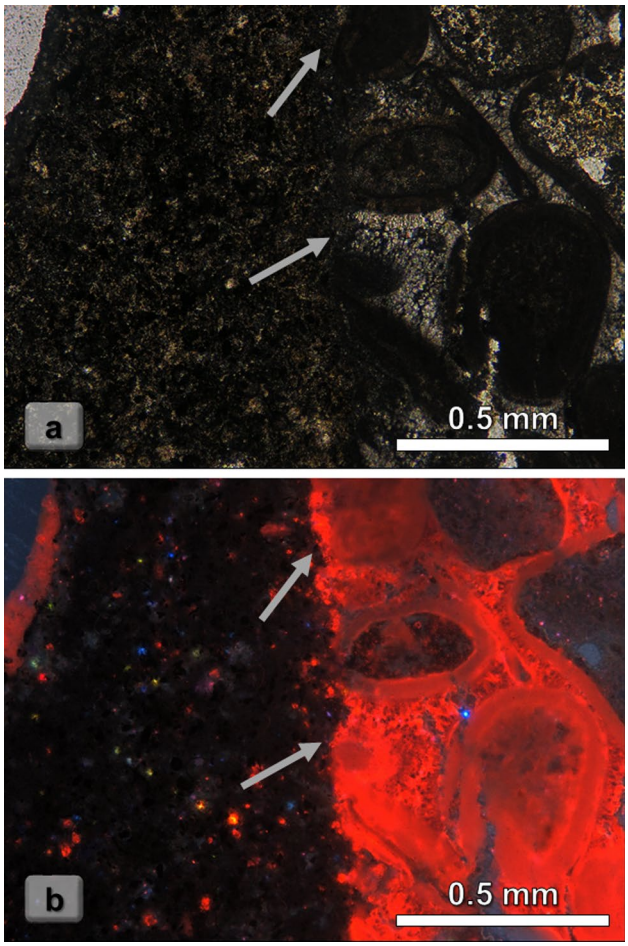

Fig. 6 Polarizing microscopic images (**a**) and cathodoluminescence microscopic picture (**b**) showing the boundary (marked by arrows) between the black weathering crust and the oolitic limestone substrate (F sample from Reims Cathedral, France)

Chemical composition

Our studies revealed that sulphate and calcium concentrations correlate well with the independently detected gypsum content (Fig. 7). The host rock samples have lower SO_4 and Ca ion concentrations (usually less than 1000 mmol/kg) (Fig. 7a) than those of the black crusts (2500–5000 mmol/kg) (Fig. 7b). Comparing the values of host rock and black crusts, it is clear that only a small proportion of SO_4 and Ca can be found in host rocks compared to black crusts. There are some exceptions (D1, D4, CZ) where these proportions are higher; only half of these concentrations were measured in the host rock (D1—crust 3500, host rock 2300 mmol/kg; D4—crust 4000, host rock 2000 mmol/kg; CZ—crust 3000, host rock 1300 mmol/kg). The extreme low values of SO_4 and Ca ion concentrations in host rocks were measured in samples D6, D7, H1, H2 (less than 200 mmol/kg) (Fig. 7a).

When gypsum content obtained by XRD is plotted against calcium concentration, two very distinct fields of samples are identified, namely black crusts and host rocks. The correlation between these two values is extremely good ($R^2 = 0.9054$) and can be described with a mathematical formula (Fig. 8a). A similar trend is observed when gypsum content is plotted against sulphate content, with an even better correlation ($R^2 = 0.9070$) (Fig. 8b). The samples are plotted along a line when calcium/sulphate content is shown in linear scale, 0 to 250,000/500,000 mg/kg. On both diagrams, host rocks represent the lower fields with lower gypsum contents (in all cases less than 50%, and usually even less than 20%) (Fig. 8).

The sulphate concentrations in the black crust have narrower ranges, while a bigger scattering is observed in the sulphate content of the host rock (Fig. 7).

Conductivity measured in solution of dissolved samples also correlates well with the gypsum content. A linear correlation was found with relatively high R-squared values ($R^2 = 0.8825$) (Fig. 9).

LA-ICP-MS analyses provide valuable information on the distribution of sulphur and lead in the host rock and black weathering crusts. The concentrations of those elements were detected along lines cross-cutting black crust host rock transitions. Our results clearly document high concentrations of lead in black crusts and a significant drop in Pb at the crust/host rock boundary (Fig. 10). In this scale, there is a transition zone between the black crust and its host rock. Comparing two samples (Fig. 10a, b and c, d), it is clear that the transitional zone is thicker for the sample from Göttingen (Fig. 10a, b). This is related to the more porous nature of the host rock and thicker alteration zone. In our study, we have found that the proportion of lead and sulphur is different for weathering crusts from different sites, but it can be different within the same city (Fig. 11). The sample which was collected from the site with a higher local SO_2 concentration (from Belgium) (Fig. 2) has higher lead concentrations than the one that was collected from lower SO_2 level site in Germany (Fig. 11).

GC–MS analyses revealed that PAH is found in all studied samples. The smallest amount of PAH was detected in a host rock sample with 0.209 mg/kg (sample D6). The highest PAH concentration was recorded in a black crust sample with 102.485 mg/kg (sample H2). When sulphate concentrations are plotted against PAH levels, it is clear that black weathering crusts are enriched both in PAHs and in sulphate (Fig. 12). The difference between the host rock samples and crust samples shows great variations. Figure 12 clearly reflects these differences, and this is probably related to differences in air pollution levels at the investigated sites, but also due to climatic differences (Table 1), with higher dissolution rates of gypsum in more humid sites.

Table 4 Main mineral phases of limestones (left) and black crusts (right) as revealed by XRD (xxx: major (60–100% mineral (either calcite or gypsum)) the values in between 80 and 100% are given in bold), xx: medium (20–60%), x: minor (5–20%) and *: trace (less than 5%)

Host rock							Black crust						
Minerals	Calcite	Gypsum	Quartz	Feldspar	Clay minerals	Micas	Minerals	Calcite	Gypsum	Quartz	Feldspar	Clay minerals	Micas
Sample codes							Sample codes						
D1-a	xx	xx	*				D1-b	x	xxx	xx			
D2-a	xxx	x	*				D2-b	x	**xxx**	x			
D3-a	xxx	*	*	*		*	D3-b	xx	xx	xx	*		*
D4-a	xx	xx	x	*			D4-b	x	xxx	x			
D5-a	xxx	x	*				D5-b	x	xxx	x	*		
D6-a	**xxx**	*	*				D6-b	x	**xxx**	x	*		
D7-a	**xxx**	x	*				D7-b	*	**xxx**	*			
H1-a	**xxx**	x	x				H1-b	x	xxx	x	*		*
H2-a	**xxx**	*	*				H2-b	*	xxx	x	*	*	
B-a	xx	xx	*				B-b	xx	xxx	x			
CZ-a	xx	xx	xx	*	*	*	CZ-b	x	**xxx**	*	*	*	*
F-a	**xxx**	*	*				F-b	xx	xx	*			
I	**xxx**	x	*										
PL-a	**xxx**	*	*				PL-b	**xxx**	x	*			

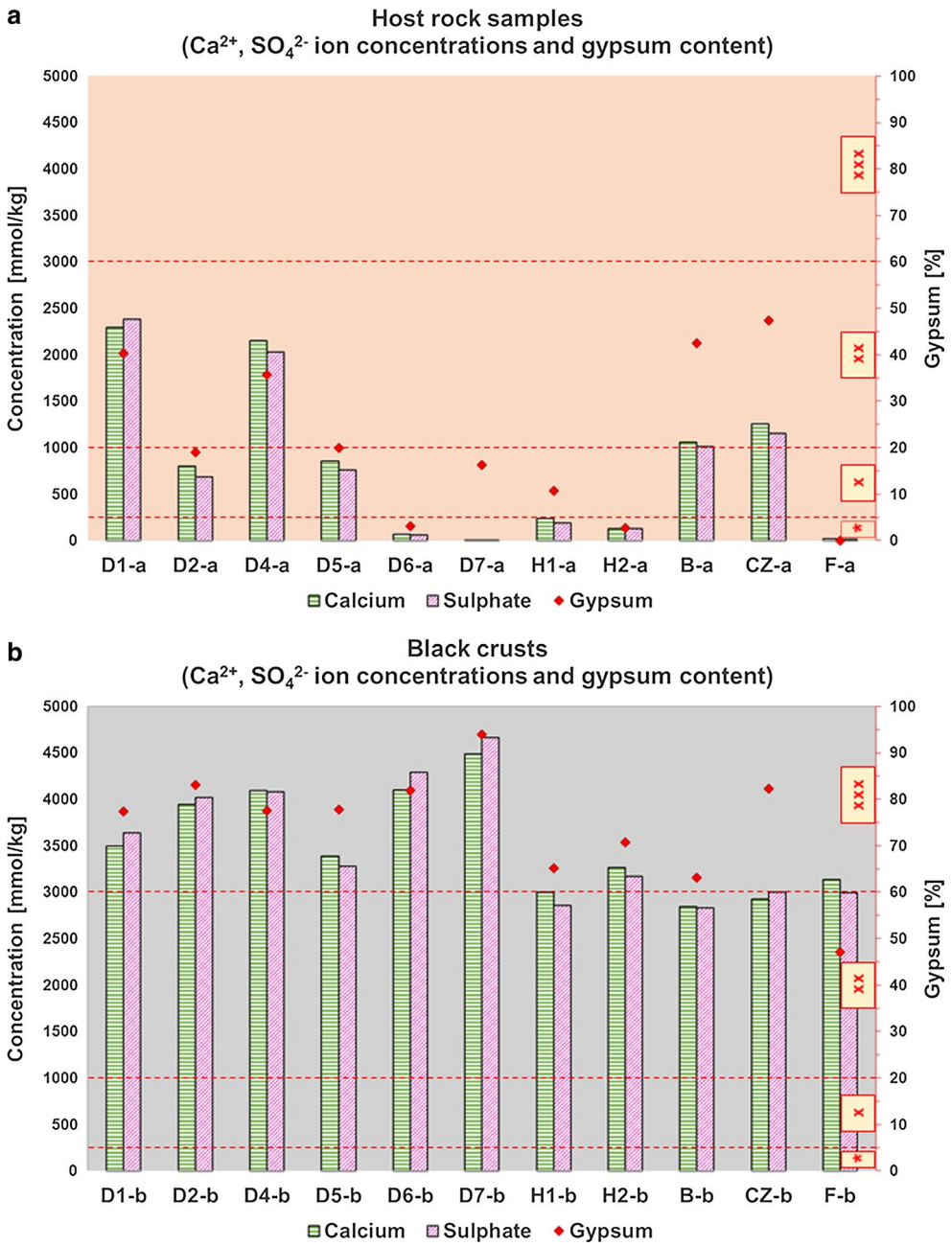

Fig. 7 Calcium and sulphate ion concentration [mmol/kg] determined by ion chromatography and gypsum content [%] determined by XRD and calculated by Rock Jock in host rock (**a**) and in black crust (**b**). Note that lower values were detected in host rock samples than in black crusts taken from the host rock. Sample codes are given in Table 3. Gypsum content—xxx: major (60–100%), xx: medium (20–60%), x: minor (5–20%) and *: trace (less than 5%) as in Table 4. (Diamonds represent calculated gypsum content)

Discussions

The upper part of framboidal black weathering crusts is covered by rosette-like gypsum crystals. This morphology was previously described for several other black crusts developed on limestone (Maravelaki-Kalaitzaki and Biscontin 1999; Török 2002; Smith et al. 2003; Török and Rozgonyi 2004; Pozo-Antonio et al. 2017), on travertine (Török 2008) or on marble (Del Monte et al. 1981, Moropoulou et al. 1998). The irregular morphology and larger surface area allows the settling of larger amount of particulate matter. It is attached to the surface, and later it is incorporated into the gypsum crust. The entrapment mechanism of particulates at irregular surfaces of gypsum has been described previously using chamber tests (Ausset et al. 1999) or samples taken from buildings (Amoroso and Fassina 1983). These particulates

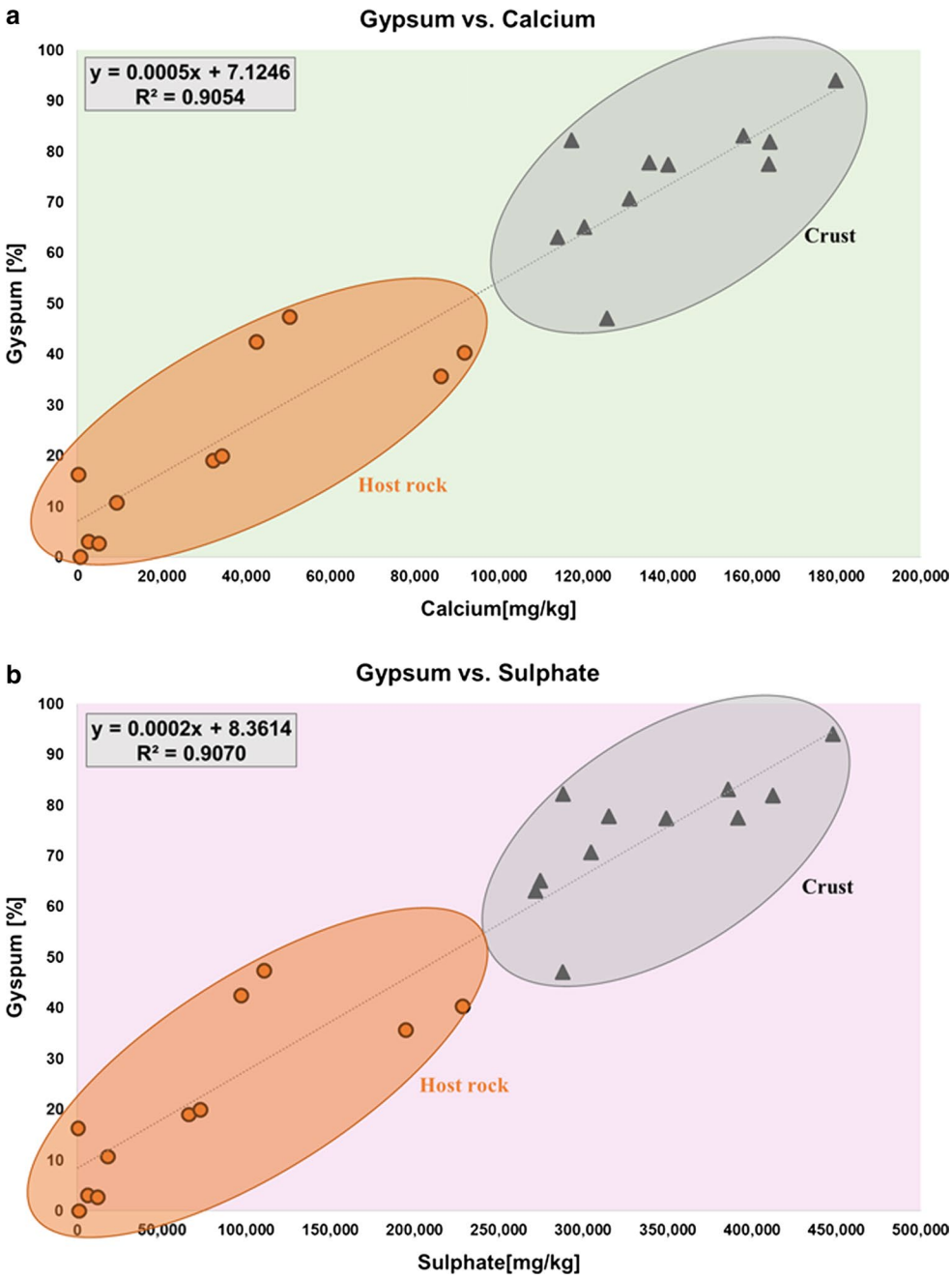

Fig. 8 Correlation between gypsum content [%] determined by XRD and calculated by Rock Jock and **a** calcium ion concentration [mg/kg] **b** sulphate ion concentration [mg/kg] determined by ion chromatography

provide information on the nature of pollution and can indicate industrial or rural origin (Török et al. 2011) or can be the indication of past pollution levels (Fobe et al. 1995). Laminar black crusts display gypsum crystals that are partly dissolved. This is related to the partial exposure of rain wash, which was also reported previously (Amoroso and Fassina 1983; Maravelaki-Kalaitzaki and Biscontin 1999; Török and Rozgonyi 2004; De Kock et al. 2017).

Our analyses suggest that there is no morphological difference between the surfaces of the crusts developed on limestone, travertine or marble if the substrate is similarly exposed. This means that exposure controls the morphology of the black crusts (Amoroso and Fassina 1983) on the studied carbonates. The differences are better explained at the substrate/crust transition zone. The contact between the carbonate substrate and the crust was studied in cross sections. Previous studies (Török et al. 2011) revealed that at thin laminar crusts a transitional zone exists between porous host limestone and crust, whereas a sharp contact was observed between framboidal black crusts and host rock (Török et al. 2011; Pozo-Antonio et al. 2017). The sharp zone between black crust and non-porous limestone was also documented by CL microscopy (Fig. 6). The black colour of the crust is related to particulate matter which is clearly visible under

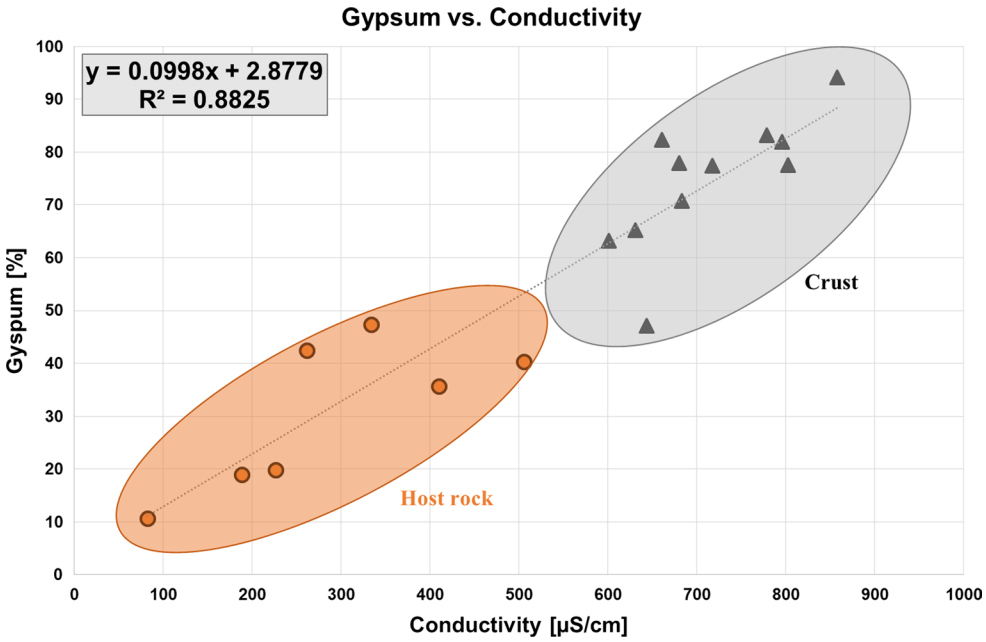

Fig. 9 Correlation between gypsum content [%] determined by XRD and calculated by Rock Jock and conductivity [µS/cm]

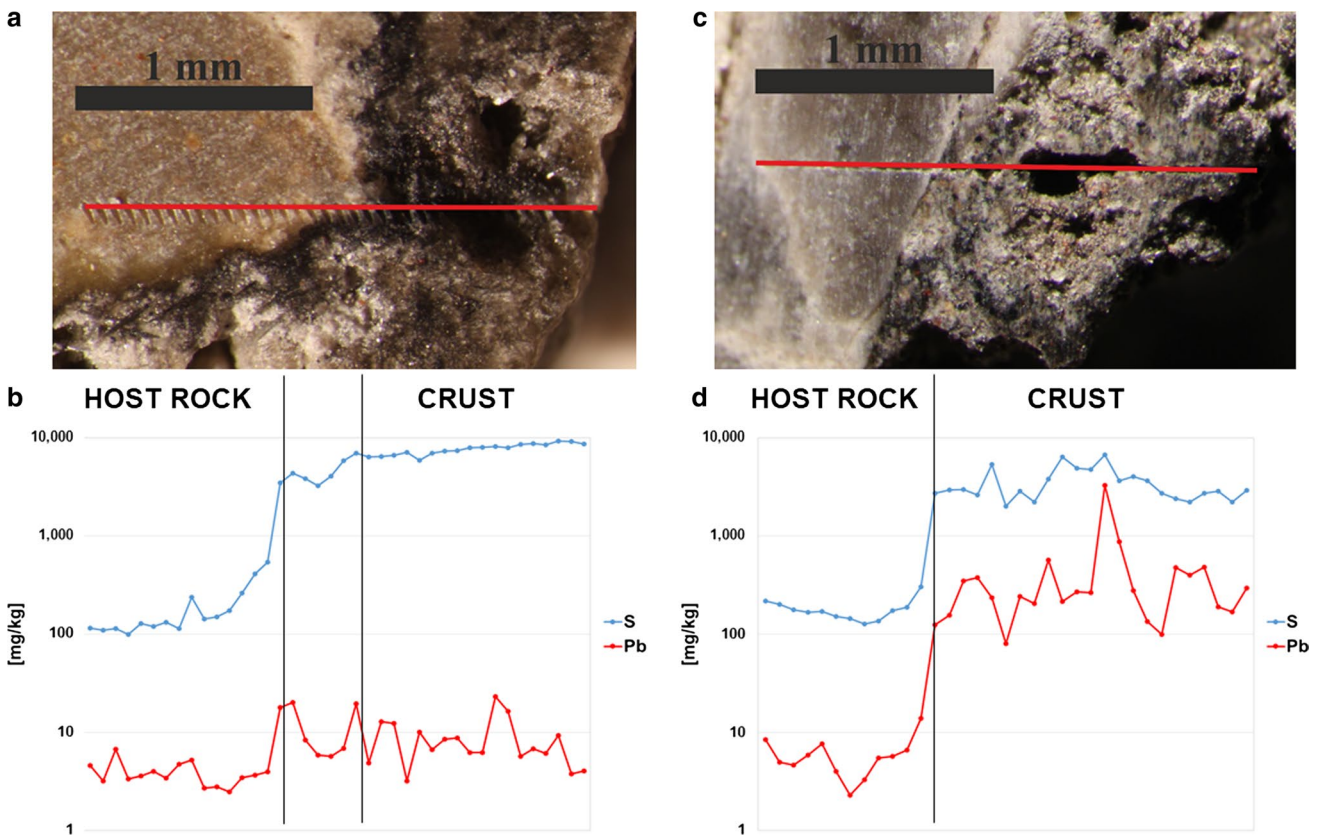

Fig. 10 Distribution of lead (red) and sulphur (blue) concentration [mg/kg] determined by LA-ICP-MS in black weathering crusts developed on limestone in Germany (sample D4 from Göttingen—**a**, **b**) and in Belgium (sample B from Liege—**c**, **d**)

the microscope (Fig. 6a). Besides black particles, silt-sized quartz grains are also visible. This incorporation of wind-blown mineral grains into the black crust is known for many years (Amoroso and Fassina 1983). Thus, the quartz content (always less than 15%) can be attributed to wind-driven mineral grains and might represent the minerals of the hinterland

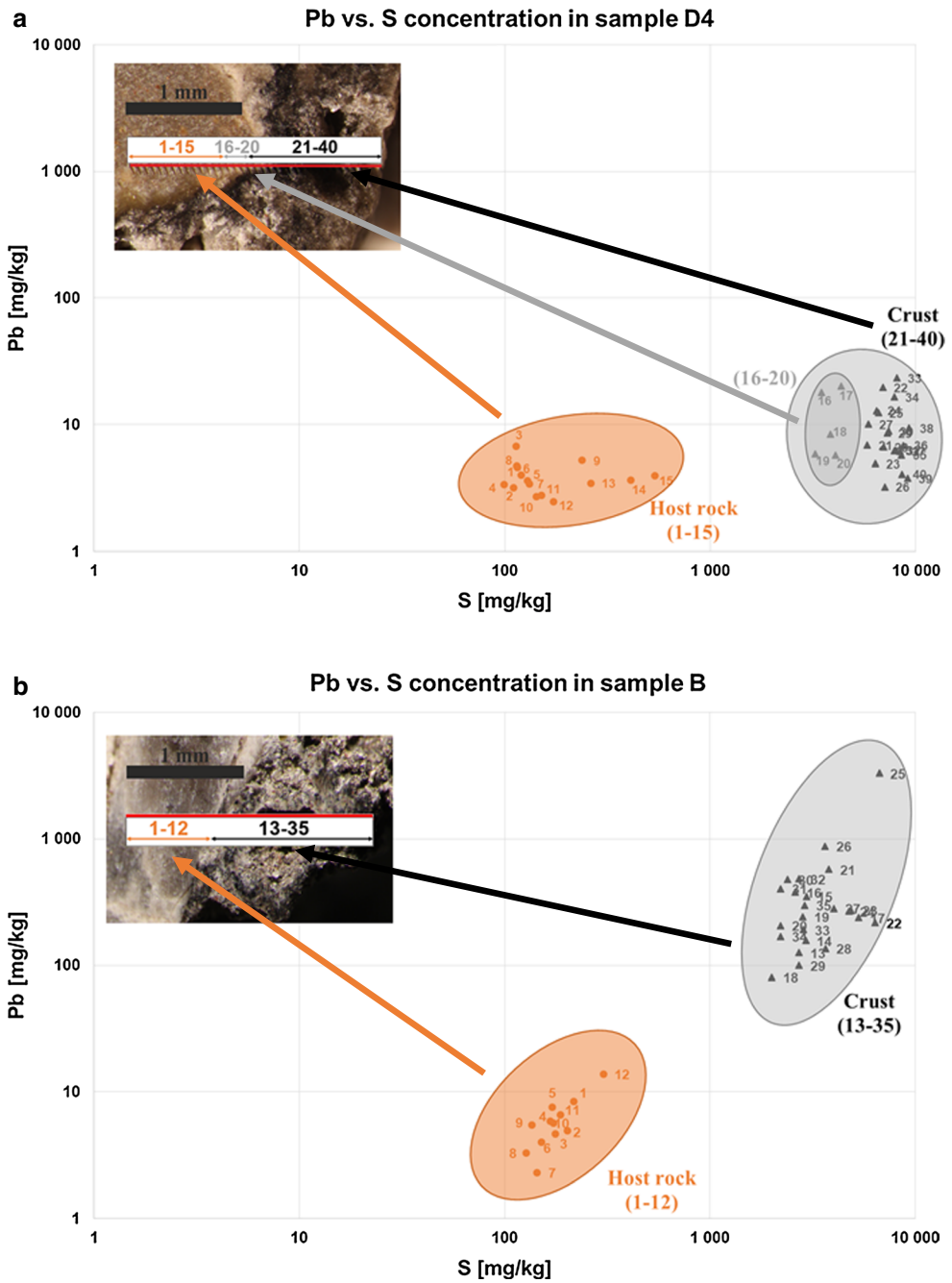

Fig. 11 Correlation between lead and sulphur concentrations determined by LA-ICP-MS (Pb and S concentrations are in mg/kg and shown on logarithmic scale). Measured values of sample D4 (**a**) and B (**b**) are significantly separated, the two groups are host rock and crust. Numbers (**a** 1–40, **b** 1–35) in the data fields refer detection points of LA-ICP-MS measurements along the line

(Smith et al. 2003; Török et al. 2011) or particles originating from street dust/traffic (Kim et al. 2016). Feldspar, which is not an authigenic mineral of the host carbonates, is also a mineral that is most likely of wind-driven origin. To the contrary, feldspar is an important mineral phase in trachyte and, thus, its presence in the black crust of trachyte (Graue et al. 2013; Germinario et al. 2017) could have also local sources.

Ion chromatographic analyses with combination of XRD provide valuable results when the origin of gypsum is questioned (Török et al. 2011; Graue et al. 2013). Sulphate content is strongly linked to gypsum (Fig. 7). No other sulphates than Ca was found with XRD, which indicates that all the sulphates are found in the form of gypsum in the studied crusts. Conductivity also has a strong link with ionic content of the solution, i.e. sulphate content (gypsum content vs.

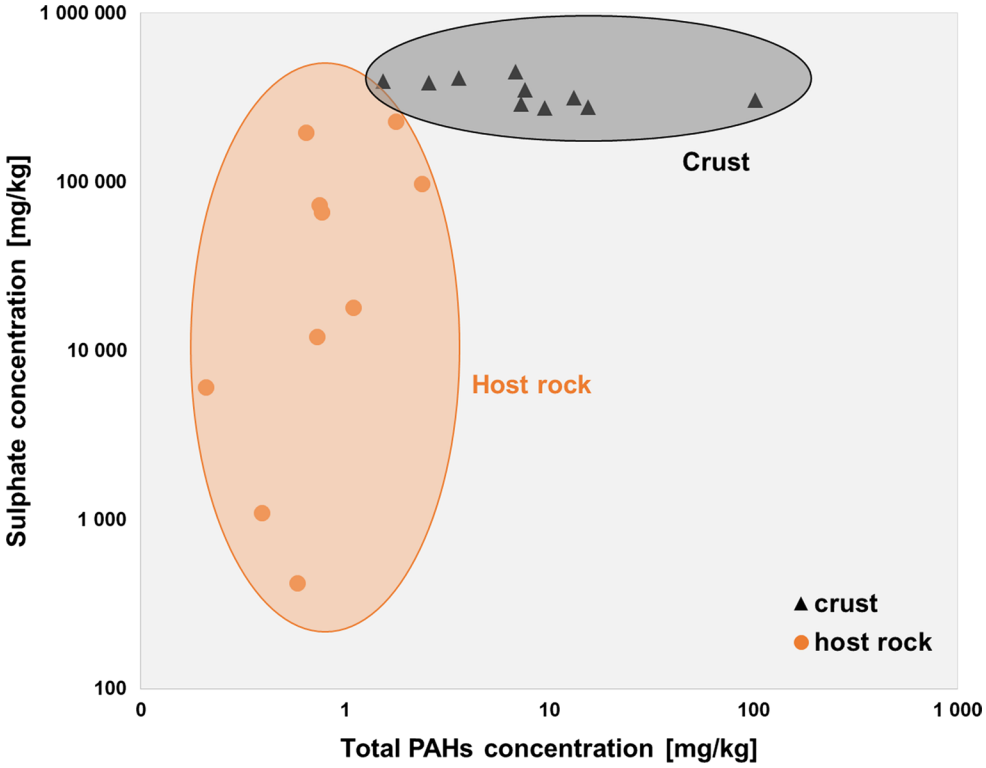

Fig. 12 Total PAH concentrations (summarizing the concentration values of the measured 22 PAH compounds) [mg/kg] determined by GC–MS versus water-soluble sulphate content [mg/kg] determined by ion chromatography of studied samples. The graph shows the difference in composition of black crust and host rock

sulphate content, Fig. 9). This is related to gypsum content since no significant amount of other minerals having high solubility was found by XRD analyses (Table 5). This means that other soluble salts play a negligible role, similarly to the findings of McAlister et al. 2008. The good solubility is also reflected on the laminar black samples where dissolved gypsum crystals are visible (Török and Rozgonyi 2004).

The correlation between gypsum content and sulphate reflects that the formation of gypsum crystals is strongly linked to air pollution. When gypsum concentration (Fig. 7) and national SO_2 emissions (Table 2) are compared, it is clear that samples taken from countries where "high SO_2 emission" was recorded has not necessarily higher gypsum concentration. It suggests that local sources contribute the SO_2 levels. It has been also demonstrated previously that urban and rural black crusts have different compositions with higher gypsum content in the urban or industrialized sites (Sánchez et al. 2011; Török et al. 2011; Graue et al. 2013).

In terms of mineralogy of substrate, the same trend was observed in samples of black crusts on limestone samples (Török et al. 2011) or in results of weathering crusts developed on trachyte (Graue et al. 2013; Germinario et al. 2017). Since samples of different carbonate host rocks such as limestone, travertine or marble were analysed, these results and the previously published ones (Török et al. 2011) clearly indicate that gypsum formation in polluted atmosphere is controlled by the presence of carbonate (i.e. calcite) (Moropoulou et al. 1998; Török 2002; Gavino et al. 2004). The proportion of gypsum in the crust developed on carbonates is different. These differences can be attributed on the one hand to the differences of the properties of substrate (porosity, solubility, etc.) (Török et al. 2011), on the other hand to the differences of local SO_2 levels (Amoroso and Fassina 1983) and to micro-climatic conditions (precipitation, exposure of the stone surface, etc.) (Slezakova and Castro 2011; Pozo-Antonio et al. 2017). The high sulphate concentrations of the black crust samples mark the similarities in the mechanism of black weathering crust formation of carbonate substrates being exposed to different but SO_2-polluted environments.

Our results clearly document that there is high concentrations of lead in black crusts. The source of lead is suggested to be the former use of leaded petrol in Europe. In Table 5, documented high concentrations suggest that lead is still present in the urban environment many years after the ban of leaded petrol in Europe, as it has been also shown by previous studies (Sánchez et al. 2011; Török et al. 2011; Graue et al. 2013). There is a significant drop in Pb at the crust/host rock boundary similarly to previous studies on black crusts (Török et al. 2011; Graue et al. 2013; La Russa

Table 5 Concentrations of lead (Pb) detected mean values [ppm] in the black crusts on various stone types (trachyte, limestone, travertine, marble, sandstone and calcarenite) from different urban sites in Europe between 2003 and 2017

Location		Lead (Pb) [ppm]	Stone substrate	References
City	Country			
Padua	Italy	22	Trachyte	Germinario et al. (2017)
Cologne	Germany	1849	Trachyte	Graue et al. (2013)
Xanten	Germany	1944	Trachyte	Graue et al. (2013)
Halle	Germany	2000	Limestone	Török et al. (2011)
Göttingen	Germany	9	Limestone	This paper
Braunschweig	Germany	196	Limestone	This paper
Halberstadt	Germany	120	Limestone	This paper
Budapest	Hungary	159	Limestone	This paper
Budapest	Hungary	1000	Limestone	Török et al. (2011)
Bari	Italy	40	Marble	This paper
Milan	Italy	883	Marble and limestone	Sabbioni (2003)
Venice	Italy	123	Marble and limestone	Sabbioni (2003)
Rome	Italy	532	Marble and limestone	Sabbioni (2003)
Bologna	Italy	427	Marble and limestone	Sabbioni (2003)
Eleusis	Greece	300	Marble and limestone	Sabbioni (2003)
Katowice	Poland	110	Travertin	This paper
Reims	France	48	Limestone	This paper
Liege	Belgium	408	Limestone	This paper
Brussels	Belgium	516	Sandstone and calcarenite	Sabbioni (2003)
Bologna	Italy	160	Sandstone and calcarenite	Sabbioni (2003)
Granada	Spain	40	Sandstone and calcarenite	Sabbioni (2003)

et al. 2017) in one sample (Fig. 10 c, d), while in the other sample the lead concentration in the crust and host rock is very similar (Fig. 10 a, b). It can be attributed to the different exposure to pollutants at the two sampling sites, namely the sample where the lead concentration is similar in the crust and host rock is from Göttingen (D4), with low traffic load till 2000 (leaded petrol use), while Belgian sample (B) is from traffic-loaded city of Liege. Lead is indicative for leaded petrol and can provide valuable information on the mobility of pollutants; a transfer from the crust of the stone surface to the deeper layers of the substrate was shown by Török et al. (2011). The presence of lead in the host rock indicates the high mobility of lead and possible migration within the pore system. The equally high sulphur concentrations in both samples (Figs. 10, 11) suggest that gypsum formation is not linked to transportation-related pollutants, but industry-driven or heat-driven SO_2 levels. It can be also suggested that longer term exposure to SO_2 (even to lower levels of SO_2) can lead to the formation of gypsum at less industrialized sites, too.

The differences in the trends of sulphur and lead can be attributed to the presence of particulate matter in the crust. It has been long known (Amoroso and Fassina 1983) that sulphur in weathering crusts is associated with gypsum.

On the other hand, the higher proportions of lead in the Belgian samples are clearly associated with higher amounts of PM produced by vehicle exhausts in the industrialized Belgian city. Thus, lead is derived from leaded fuels and incorporated into gypsum. The proportion of lead vs. sulphur is different in the studied German and Belgian samples, but black crusts and host rocks represent two distinct fields on these graphs (Fig. 11).

PAHs have been found in all tested samples in which compounds are indicatives of air pollution, improper combustion and related to the burning of fossil fuels (Lima et al. 2005) or other organic substances (Simoneit 2002) in the urban environment. Thus, these compounds are linked to human activity in urban areas and mostly linked to particulate matter. Relatively high concentration of PAH in crust (Fig. 12) suggests that gypsum crust encloses particulates. Thus, PAH content can be correlated with gypsum/sulphate concentration. Török et al. 2011 also correlated PAHs with sulphur finding slightly different results. Later, Graue et al. 2013 demonstrated the presence of PAH not only in the black weathering crusts of carbonates, but also in crusts found on trachyte and sandstone. These previous studies are in agreement with our findings that PAH found in black crusts marks air pollution. It has been also noted that PAH can be used as tracer of present and past pollution levels not only in weathering crusts, but also in lake sediments (Warner et al. 2016).

Conclusions

The analytical results of black crusts and host rocks collected from seven European countries clearly indicate that gypsum accumulates not only in black crusts, but also the host rock contains small amount of it. The gypsum content of black crusts is 4–5 times larger than that of the host rock.

Accessory minerals, such as quartz, further accumulate in the crust, suggesting the presence of wind-driven particulates.

SEM analyses revealed that organic carbon and spherical fly ash particles are present on the top of the framboidal crusts, and these particles are entrapped in between gypsum crystals.

The cathodoluminescence microscopy of studied host rocks and black crusts is markedly different, namely the former ones have bright orange luminescence, while black crusts are non-luminescent with a few bright orange or violet-blue spots of wind-blown dust.

There is a strong linear correlation (high *R*-square values) between the gypsum content determined by XRD and the water-soluble sulphate calcium content. The highest values are found in black crusts. Additionally, conductivities of water-extracted black crusts and host rocks correlate well with their gypsum content, since no other highly soluble salts were detected in the samples by XRD.

LA-ICP-MS analyses indicate that lead accumulates in the black crusts, and its concentration suddenly drops at the crust/stone interface in samples that were exposed to higher traffic in the past. Sulphur shows the same trend, but it seems that the proportion of sulphur and lead is different for different samples.

All the studied black crusts and host rocks contain polycyclic aromatic hydrocarbons (PAH). PAH content of black crusts is higher than that of the underlying host rocks, but the discrepancy between the measured PAH values of crust and host rock is very different from sample to sample.

Air pollution levels are not reflected in the gypsum content of black weathering crusts. It seems that the persistent and carcinogenic pollutants PAH and Pb reflect present and past air pollution levels much better.

Acknowledgements The financial support of Deutsche Bundesstiftung Umwelt (DBU, 30016/686) and Hungarian National Research, Development and Innovation (NKFI) Fund (K 116532) is appreciated. We are grateful for the constructive discussions on analytical techniques and results with István Dunkl. We thank a lot Klaus Wemmer, who helped with the identification of mineral phases during XRD analyses. The help of Prof. Dr. Bernhard Schulz, Sabine Haser in SEM analyses is appreciated. We are grateful to Mechthild Rittmeier and Wiebke Warner for GC–MS and IC analyses, Klaus Simon for LA-ICP-MS analyses, Harald Tonn and Alfons van den Kerkhof for microscopy. We would like to thank the samples from France and Italy for Patricia Vazquez and Luigi Germinario.

References

Amoroso GG, Fassina V (1983) Stone decay und conservation. Elsevier, Amsterdam, pp 1–453

Antill SJ, Viles HA (1999) Deciphering the impacts of traffic on stone decay in oxford: some preliminary observations from old limestone walls. In: Jones MS, Wakefield RD (eds) Aspects of stone weathering, decay and conservation. Imperial College Press, London, pp 28–42

Ausset P, Bannery F, Lefèvre RA (1992) Black-crust und air microparticles contents at Saint-Trophime, Arles. In: Delgado Rodriguez J, Henriques F, Termo Jeremias F (eds) 7th International congress on deterioration und conservation of stone, Lisbon, pp 325–334

Ausset P, Del Monte M, Lefèvre RA (1999) Embryonic sulfated black crusts on carbonate rocks in atmospheric simulation chamber and in the field: role of carbonaceous fly-ash. Atmos Environ 33:1525–1534

Baboian R (ed) (1986) Materials degradation caused by acid rain. Symposium series 318. American Chemical Society, Washington, DC

Bonazza A, Sabbioni C, Ghedini N, Favoni O, Zappia G (2004) Carbon data in black crusts on European monuments. In: Saiz-Jimenez C (ed) Air pollution und cultural heritage. Taylor & Francis, London, pp 39–46

Bonazza A, Sabbioni C, Ghedini N (2005) Quantitative data on carbon fractions in interpretation of black crusts and soiling on European built heritage. Atmos Environ 39:2607–2618

Bonazza A, Brimblecombe P, Grossi CM, Sabbioni C (2007) Carbon in black crust from the tower of London. Environ Sci Technol 41:4199–4204

Brimblecombe P (1987) The big smoke: a history of air pollution in London since medieval times. Methuen, London, p 185

Brimblecombe P (1996) Air composition und chemistry (Cambridge environmental chemistry series), 2nd edn. Cambridge University Press, Cambridge, p 253

Brimblecombe P (2003) The effects of air pollution on the built environment. Air pollution reviews, vol. 2. Imperial College Press, London

Camuffo D (1998) Microclimate for cultural heritage. Elsevier, Amsterdam, p 432

CAN (2015) The coal map of Europe. http://coalmap.eu/#/. Accessed Oct 2016

Charola AE (2001) Review of the literature on the topic of acidic deposition on stone. US/ICOMOS Sci J 3:19–58

Charola AE, Ware R (2002). Acid deposition und the deterioration of stone: a brief review of a broad topic. In: Siegesmund S, Vollbrecht A (eds.) Natural stone, weathering phenomena, conservation strategies und case studies. Geological Society, London, Special publication 205, p 393–406

CHMI (2017) Český Hydrometeorologický Ústav. http://portal.chmi.cz/. Accessed Apr 2017

Climate-Data (2017) Klimadaten für Städte Weltweit. https://de.climate-data.org/. Accessed Apr 2017

De Kock T, Van Stappen J, Fronteau G, Boone M, De Boever W, Dagrain F, Silversmit G, Vincze L, Cnudde V (2017) Laminar gypsum crust on lede stone: microspatial characterization and laboratory acid weathering. Talanta 162:193–202

Del Monte M, Sabbioni C, Vittori O (1981) Airborne carbon particles und marble deterioration. Atmos Environ 15:645–652

Derbez M, Lefèvre RA (1996) Le contenu microparticulaire des croûtes gypseuses de la Cathédrale Saint-Gatien de Tours: comparaison avec l'air et la pluie. In: Riederer J (ed) Proceedings of the 8th international congress on deterioration and conservation of stone, Möller, Berlin, pp 359–370

DWD—Deutscher Wetterdienst (2016) Wetter und Klima. https://de.climate-data.org/. Accessed Oct 2016

Eberl DD (2003) User's guide to RockJock—a program for determining quantitative mineralogy from powder X-ray diffraction data. U.S. Geological Survey Open-File Report 2003-78. https://pubs.usgs.gov/of/2003/of03-078/

EEA—EU European Environment Agency (2016a) Air pollutant emissions data. https://www.eea.europa.eu/data-and-maps/dashboards/air-pollutant-emissions-data-viewer. Accessed Dec 2016

EEA—EU European Environment Agency (2016b). SO_2 interactive maps. http://www.eea.europa.eu/themes/air/interactive/so2. Accessed Dec 2016

Esbert RM, Diaz-Pache F, Alonso FJ, Ordaz J, Wood GC (1996) Solid particles of atmospheric pollution found on the Hontoria limestone of Burgos Cathedral (Spain). In: Riederer J (ed) Proceedings of the 8th international congress on deterioration and conservation of stone, Möller, Berlin, pp 393–399

Fitzner B, Heinrichs K, Kownatzki R (1996) Weathering forms: classification und mapping. In: Snethlage R (ed) Denkmalpflege und Naturwissenschaft, Natursteinkonservierung I. Verlag Ernst & Sohn, Berlin, pp 41–88

Fobe B, Vleugels GJ, Roekens EJ, Hermosin B, Ortega-Calvo J, Del Junco AS, Van Grieken R, Saiz-Jimenez C (1995) Organic and inorganic compounds in limestone weathering crusts from cathedrals in southern and western Europe. Environ Sci Technol 29:1691–1701

Gavino M, Hermosin B, Vergès-Belmin V, Nowik W, Saiz-Jimenez C (2004) Composition of black crust from the Saint Denis Basilica, France as revealed by gas chromatography—mass spectrometry. J Sep Sci 27:513–523

Germinario L, Siegesmund S, Maritan L, Simon K, Mazzoli C (2017) Trachyte weathering in the urban built environment related to air quality. Herit Sci 5:44

Graue B, Siegesmund S, Oyhantcabal P, Naumann R, Licha T, Simon K (2013) The effect of air pollution on stone decay: the decay of the Drachenfels trachyte in industrial, urban, and rural environments—a case study of the Cologne, Altenberg and Xanten cathedrals. Environ Earth Sci 69:1095–1124

Grün R (1931) Die Verwitterung von Steinen. Die Denkmalpflege 33:168–183

Hildemann LM, Klinedinst DB, Klouda GA, Currie LA, Cass GR (1994) Sources of urban contemporary carbon aerosol. Environ Sci Technol 28:1565–1576

ICOMOS (2008). Illustrated glossary on stone deterioration patterns. In: Vergès-Belmin V (ed) ICOMOS International Scientific Committee for Stone, Ateliers 30 Impression, Champigny/Marne, France

Kaiser E (1910) Wetterbestätigkeit einer Reihe von Kalksteinen mit besonderer Berücksichtigung der Verhältnisse am Kölner Dom. Unpupl. Report, Gießen

Kieslinger A (1932) Zerstörung an Steinbauten—Ihre Ursachen und ihre Abwehr. Verlag Deuticke, Leipzig-Wien, p 346

Kim BM, Seo J, Kim JY, Lee JY, Kim Y (2016) Transported versus local contributions from secondary and biomass burning sources to PM2.5. Atmos Environ 144:24–36

Klemm W, Siedel H (2002) Evaluation of the origin of sulphate compounds in building stone by sulphur isotope ratio. In: Siegesmund S, Weiss TS, Vollbrecht A (eds.) Natural stones, weathering phenomena, conservation strategies and case studies. Geological Society, London, Special Publications 205, pp 419–429

La Russa MF, Fermo P, Comite V, Belfiore CM, Barca D, Cerioni A, De Santis M, Barbagallo LF, Ricca M, Ruffolo SA (2017) The Oceanus statue of the Fontana di Trevi (Rome): the analysis of black crust as a tool to investigate the urban air pollution and its impact on the stone degradation. Sci Total Environ 593–594:297–309

Lima AL, Farrington JW, Reddy CM (2005) Combustion-derived polycyclic aromatic hydrocarbons in the environment—a review. Environ Forensics 6:109–131

Maravelaki-Kalaitzaki P, Biscontin G (1999) Origin, characteristics and morphology of weathering crusts on Istria stone in Venice. Atmos Environ 33:1699–1709

McAlister JJ, Smith BJ, Török Á (2006) Element partitioning and potential mobility within surface dusts on buildings in a polluted urban environment, Budapest. Atmos Environ 40:6780–6790

McAlister JJ, Smith BJ, Török Á (2008) Transition metals and water-soluble ions in deposits on a building and their potential catalysis of stone decay. Atmos Environ 42:7657–7668

Moropoulou A, Bisbikou K, Torfs K, Van Grieken R, Zezza F, Macri F (1998) Origin und growth of weathering crusts on ancient marbles in industrial atmosphere. Atmos Environ 42:7657–7668

Neuser RD, Bruhn F, Götze J, Habermann D, Richter DK (1995) Kathodolumineszenz: Methodik und Anwendung. Zentralblatt für Geologie und Paläontologie Teil I, H.1/2, 287-306

Pozo-Antonio JS, Pereira MFC, Rocha CSA (2017) Microscopic characterisation of black crust on different substrates. Sci Total Environ 584–585:291–306

Price CA (1996) Stone conservation. An overview of current research. Research in Conservation, Getty Conservation Institute, Los Angeles

Rodriguez-Navarro C, Sebastian E (1996) Role of particulate matter from vehicle exhaust on porous building stones (limestone) sulfation. Sci Total Environ 187:79–91

Rosvall J, Aleby S (eds) (1988) Safeguarding our architechtural heritage. Elsevier, Amsterdam

Sabbioni C (1995) Contribution of atmospheric deposition to the formation of damage layers. Sci Total Environ 167:49–55

Sabbioni C (2003) Mechanism of air pollution damage to stone. In: Brimblecombe P (ed) The effects of air pollution on the built environment, vol 2. Air pollution reviews. World Scientific, Singapore, pp 63–106

Sánchez JS, Vidal Romaní JR, Alves C (2011) Deposition of particles on gypsum-rich coatings of historic buildings in urban and rural environments. Constr Build Mater 25:813–822

Schaffer RJ (1932) The weathering of natural building stones. His Majesty's Stationary Office, London, p 149

Siegesmund S, Török Á, Hüpers A, Müller C, Klemm W (2007) Mineralogical, geochemical und microfabric evidences of gypsum crusts: a case study from Budapest. Environ Geol 52:358–397

Simoneit BRT (2002) Biomass burning—a review of organic tracers for smoke from incomplete combustion. Appl Geochem 17:129–162

Slezakova K, Castro D (2011) Air pollution from traffic emissions in Oporto. Microchem J 99:51–59

Smith BJ, Viles HA (2006). Rapid catastrophic decay of building limestones: thoughts on causes, effects und consequences. In: Fort R, Alvarez de Buego M, Gomez-Heras M, Vazquez-Calvo C (eds) Heritage weathering und conservation. Taylor & Francis/Balkema, London I, pp 191–197

Smith BJ, Török Á, McAlister JJ, Megarry Y (2003) Observations on the factors influencing stability of building stones following contour scaling: a case study of oolitic limestones from Budapest, Hungary. Build Environ 38:1173–1183

Snethlage R (2008) Leitfaden Steinkonservierung—Planung von Untersuchungen und Maßnahmen zur Erhaltung von Denkmälern aus Naturstein. Fraunhofer IRB Verlag, Stuttgart, pp 48–76

Torfs KM, Van Grieken RE (1997) Chemical relations between atmospheric aerosols, deposition and stone decay layers on historic buildings at the Mediterranean coast. Atmos Environ 31:2179–2192

Török Á (2002) Oolitic limestone in polluted atmospheric environment in Budapest: weathering phenomena und alterations in physical properties. In: Siegesmund S, Weiss TS, Vollbrecht A (eds) Natural stones, weathering phenomena, conservation strategies und case studies. Geological Society, London, Special Publications 205, pp 363–379

Török Á (2003) Surface strength and mineralogy of weathering crusts on limestone buildings in Budapest. Building Environ 38(9–10):1185–1192

Török Á (2008) Black crusts on travertine: factors controlling development and stability. Environ Geol 56:583–594

Török Á, Rozgonyi N (2004) Mineralogy and morphology of salt crusts on porous limestone in urban environment. Environ Geol 46:333–349

Török Á, Müller C, Hüpers A, Hoppert M, Siegesmund S, Weiss T (2007) Differences in texture, physical properties und microbiology of weathering crust und host rock: a case study of the porous limestone of Budapest (Hungary). In: Prykril R, Smith JB (eds) Building stone decay: from diagnosis to conservation, Geological Society, London, Special Publications 271, pp 261–276

Török Á, Licha T, Simon K, Siegesmund S (2011) Urban and rural limestone weathering; the contribution of dust to black crust formation. Environ Earth Sci 63:675–693

Urosevic M, Yebra-Rodríguez A, Sebastián-Pardo E, Cardell C (2012) Black soiling of an architectural limestone during two-year term exposure to urban air in the city of Granada (S Spain). Sci Total Environ 414:564–575

Viles HA (1993) The environmental sensitivity of blistering of limestones walls in Oxford, England: a preliminary study. In: Thomas DSG, Allison RJ (eds) Landscape sensitivity. John Wiley, Chichester, pp 309–326

Warner W, Ruppert H, Licha T (2016) Application of PAH concentration profiles in lake sediments as indicators for smelting activity. Sci Total Environ 563–564:587–592

Wetterkontor (2016). Wetter-Rückblick—Monats-und Jahreswerte http://www.wetterkontor.de/. Accessed Oct 2016

Winkler EM (1994) Stone: Properties, durability in man's environment. Springer, New York

WMO—UN World Meteorological Organisation (2017) https://www.wmo.int/. Accessed Apr 2017